Pritvik Sinhadc

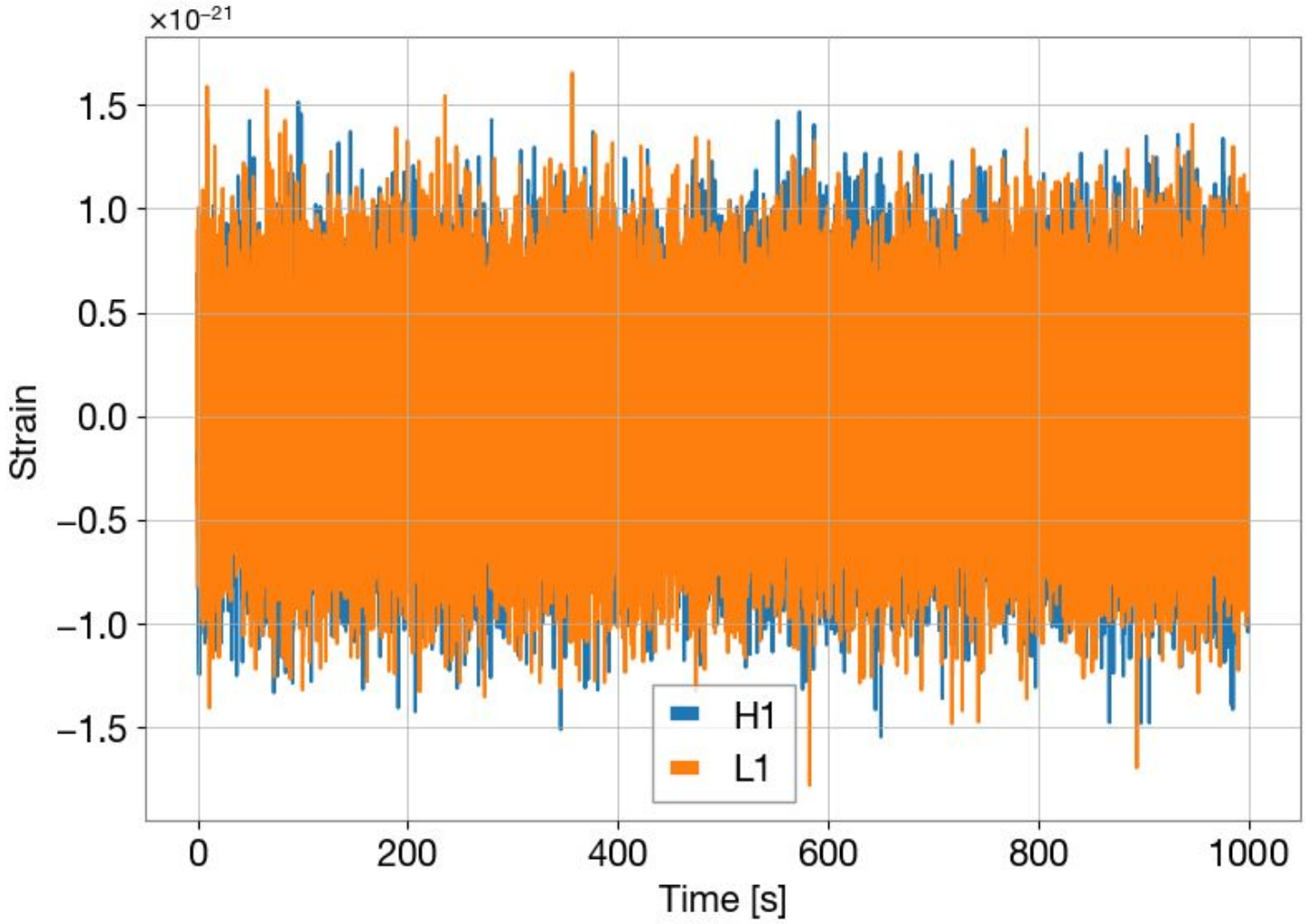

LIGO SURF PROJECT:

STOCHASTIC GRAVITATIONAL WAVE BACKGROUND

Mentors: Alan Weinstein, Patrick Meyers, Arianna Renzini

AN INTRODUCTION TO SGWB

The SGWB is a complex amalgamation of multiple sources of GWs that offer valuable insights into the evolution and history of astrophysical collisions over the universe's timespan. It is composed of unresolved waveforms, specifically the superposition of numerous GW events throughout the universe's history.

The image shows the energy density against frequency for the GWBs corresponding to BBH, BNS, NSBH merger events.

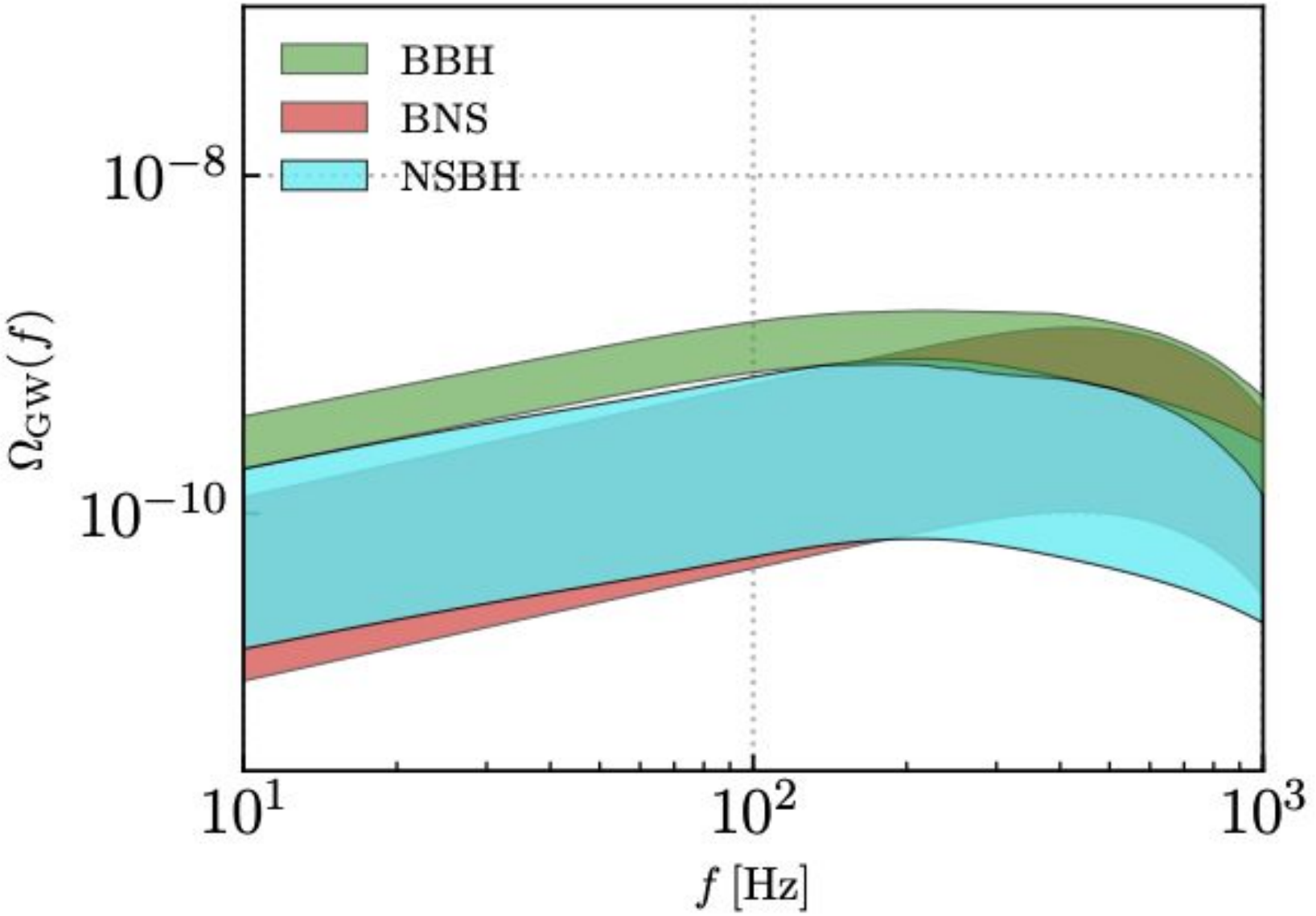

Source: *Implications for the Stochastic Gravitational-Wave Background from Compact Binary Coalescences,* B. P. Abbott et al, (LIGO Scientific Collaboration and Virgo Collaboration), *Phys. Rev. Lett,* 120, 091101, Published February 28, 2018, https://journals.aps.org/prl/abstract/10.1103/PhysRevLett.120.091101

AN INTRODUCTION TO SGWB

The image shows the energy density against frequency for the total GWB corresponding to BBH, BNS, NSBH merger events.

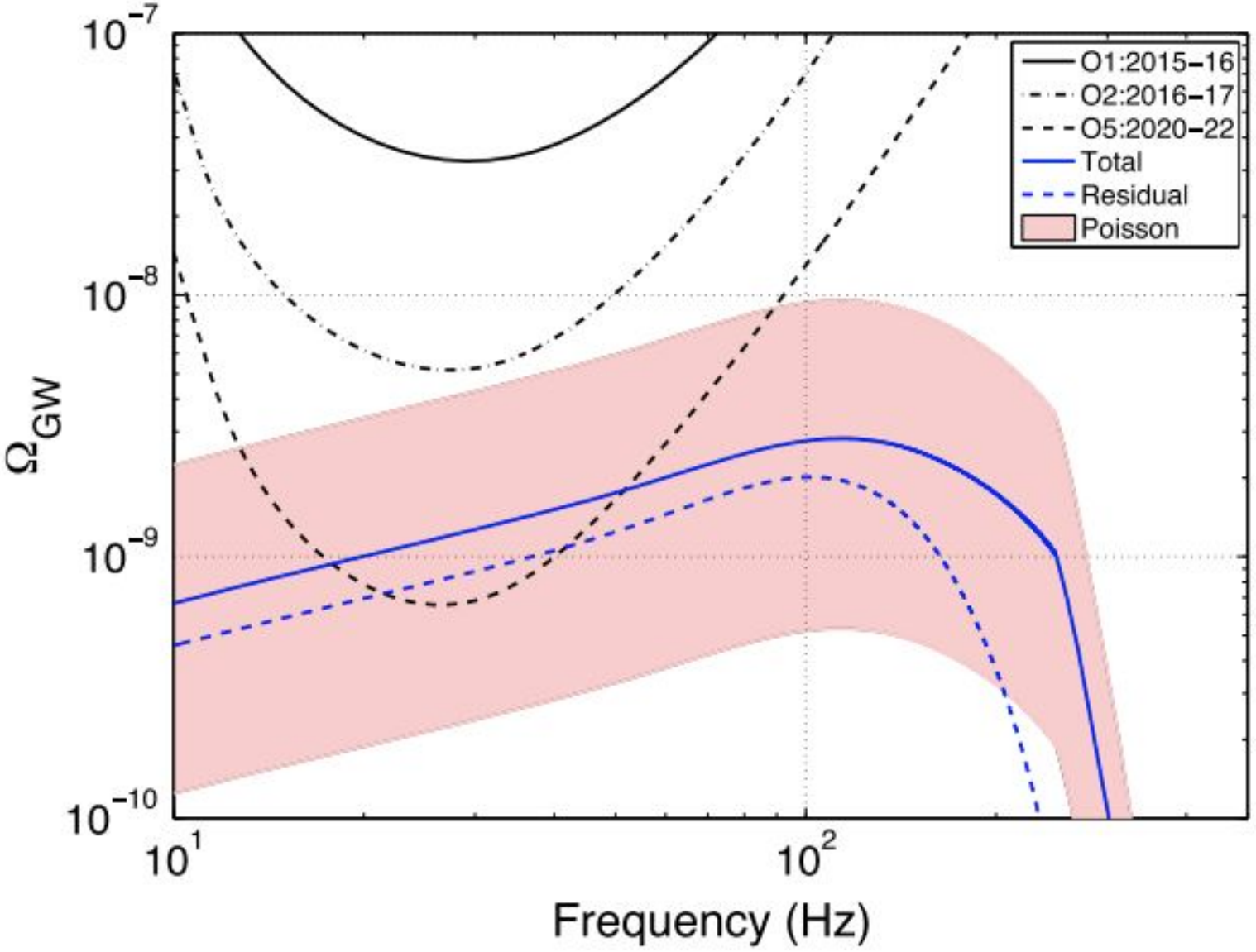

A much smaller component of the SGWB consists of a cosmological background, including the GWs predicted to be formed immediately after the Big Bang through processes during inflation. Although this portion of the SGWB is fainter, we note that its frequency lies beyond the detectable range of the ground based GW detectors, which encompass a frequency of 20-2000 Hz.

Source: GW150914: GW150914: *Implications for the Stochastic Gravitational-Wave Background from Binary Black Holes,* B. P. Abbott et al, (LIGO Scientific Collaboration and Virgo Collaboration), *Phys. Rev. Lett.* 116, 131102, Published March 31, 2016, https://journals.aps.org/prl/abstract/10.1103/PhysRevLett.116.131102;

PROJECT OBJECTIVES

1. Reproducing and comparing the estimates of the CBC merger rate and the SGWB using Monte-Carlo sampling and integration (the Regimbau method) and precomputed grids along with probability distributions (the Callister method).

2. Investigating the degree to which these estimates agree with each other and the implications of any discrepancies.

3. Studying the dependence of these estimates on uncertainties in the merger rate as a function of mass, redshift distributions of the sources, and potential anisotropies in overall source distribution.

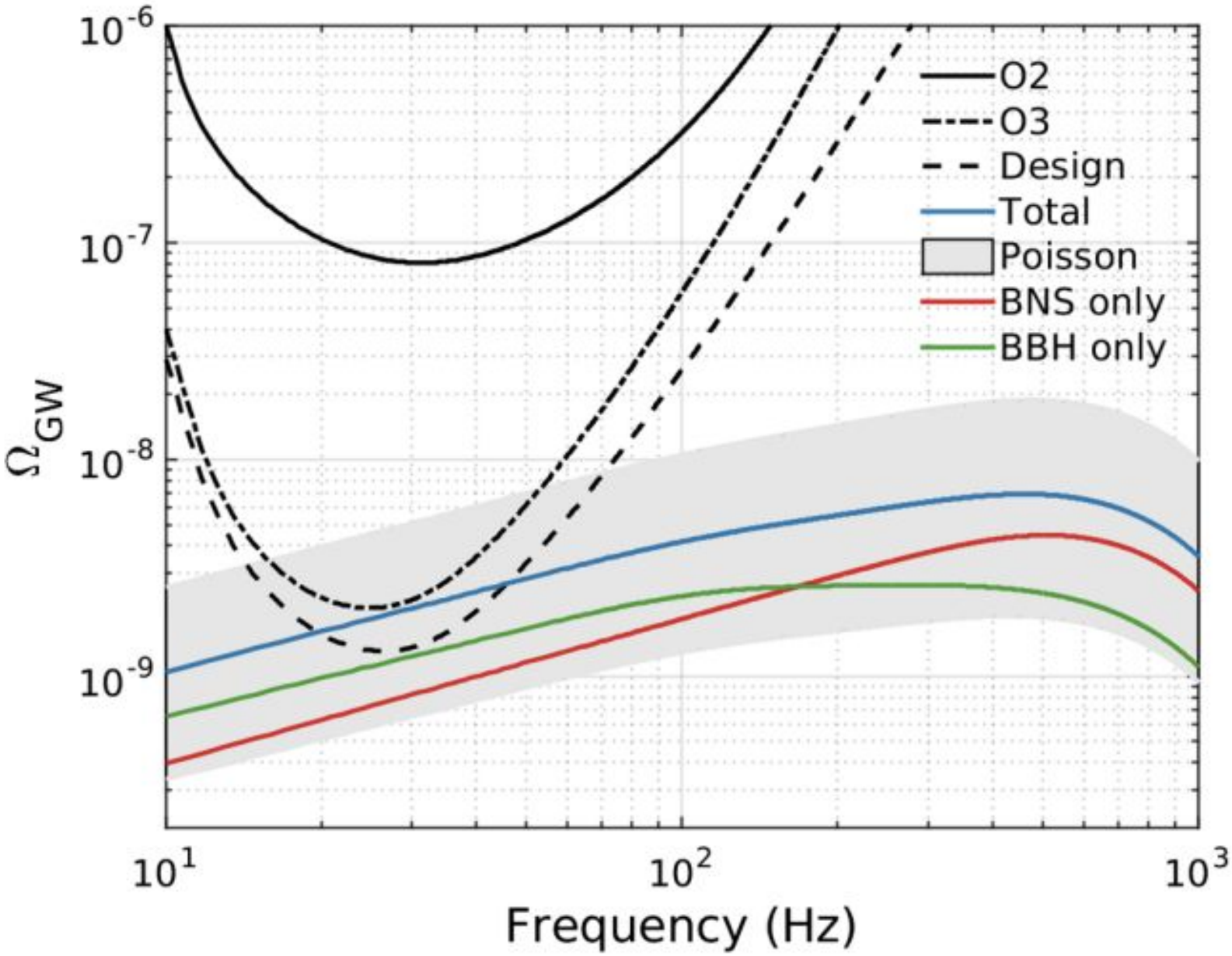

Source: GW170817: *Implications for the Stochastic Gravitational-Wave Background from Compact Binary Coalescences,* B. P. Abbott et al, (LIGO Scientific Collaboration and Virgo Collaboration), *Phys. Rev. Lett,* 120, 091101, Published February 28, 2018, https://journals.aps.org/prl/abstract/10.1103/PhysRevLett.120.091101, Fig 1

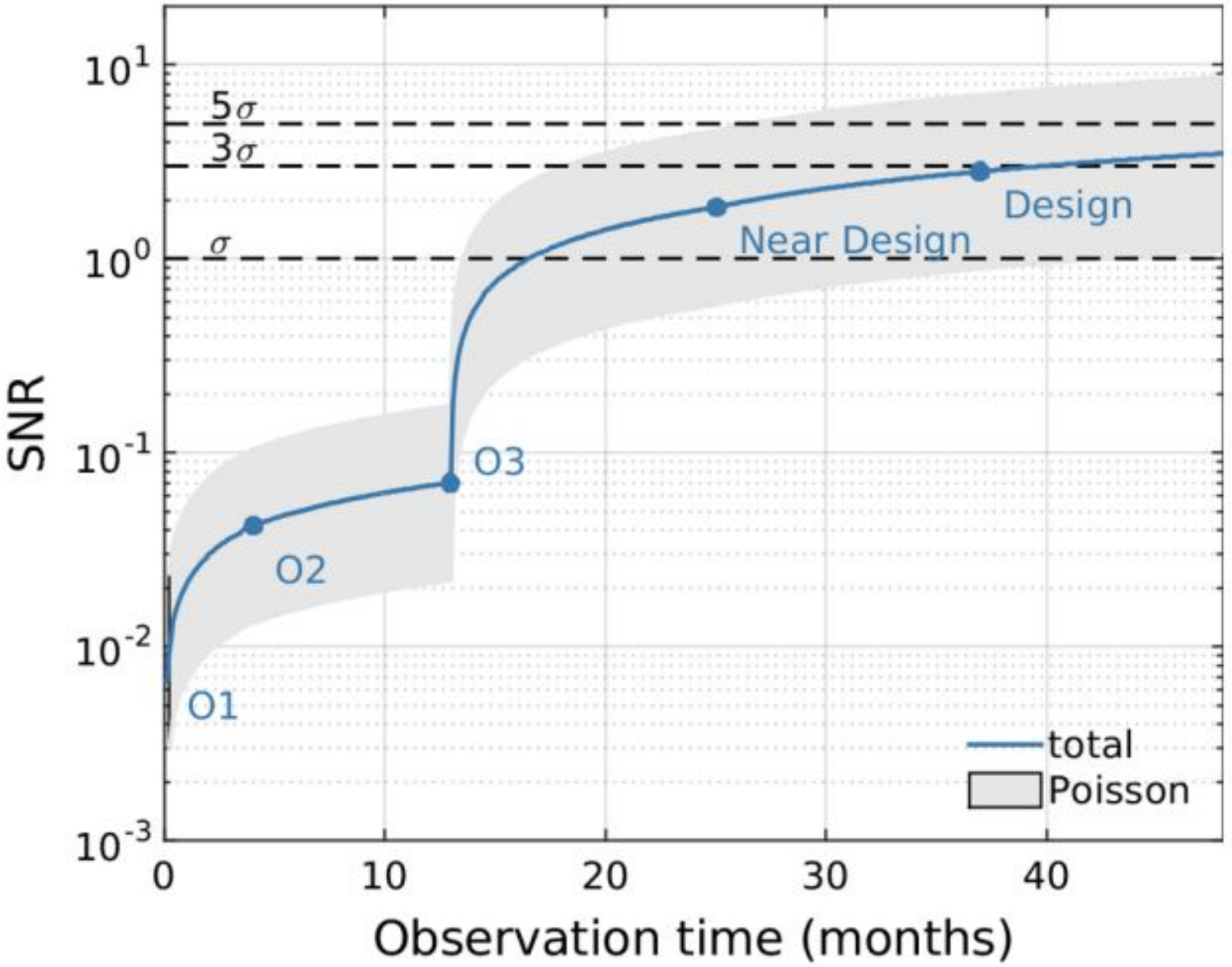

MAJOR GOAL

Assessing the impact of these uncertainties on any potential constraints that could be applied to the SGWB, including the energy density of the SGWB, contributions from different mass ranges of CBCs per frequency band, etc.

Therefore, in other words, the goal is to constrain the predictions on SGWB parameters and constrain its limits, thereby decoding how the background changes due to uncertainties in several important parameters. This will be of further aid during a future detection of the astrophysics SGWB.

Source: GW170817: *Implications for the Stochastic Gravitational-Wave Background from Compact Binary Coalescences,* B. P. Abbott et al, (LIGO Scientific Collaboration and Virgo Collaboration), *Phys. Rev. Lett,* 120, 091101, Published February 28, 2018, https://journals.aps.org/prl/abstract/10.1103/PhysRevLett.120.091101, Fig 1

OVERALL METHODOLOGY

$$\Omega_{GW}(f) = \frac{f}{\rho_c}\frac{d\rho_{GW}}{df}$$

$\rho_c = \frac{3H_0^2c^2}{8\pi G}$, or the critical energy density, $R_m(z)$ = merger rate, $H(z)$ = Hubble rate

$$\Omega_{GW}(f) = \frac{f}{\rho_c}\frac{d\rho_{GW}}{df} = \frac{f}{\rho_c}\int_0^{10}\frac{R_m(z)}{(1+z)H(z)}\left\langle\frac{dE}{df_s}\right\rangle dz$$

$f = \frac{f_s}{1+z}$, and is frequency in detector frame

$$\left\langle\frac{dE}{df_s}\right\rangle = \int dm_1 dm_2 \frac{dE}{df}(m_1, m_2; f(1+z))p(m_1, m_2)$$

$$\Omega_{GW}(f) = \frac{f}{\rho_c}\frac{d\rho_{GW}}{df} = \frac{f}{\rho_c}\int\frac{R_m(z)}{(1+z)H(z)}\left\langle\frac{dE}{df_s}\right\rangle dz = \frac{f}{\rho_c}\sum_z\left\{\frac{R_m(z)}{(1+z)H(z)}\right\}_z\left\{\left\langle\frac{dE}{df}\right\rangle\right\}_{f,z}$$

$\left\{\left\langle\frac{dE}{df}\right\rangle\right\}_{f,z}$ is the population averaged energy spectrum dependent on frequency and redshift

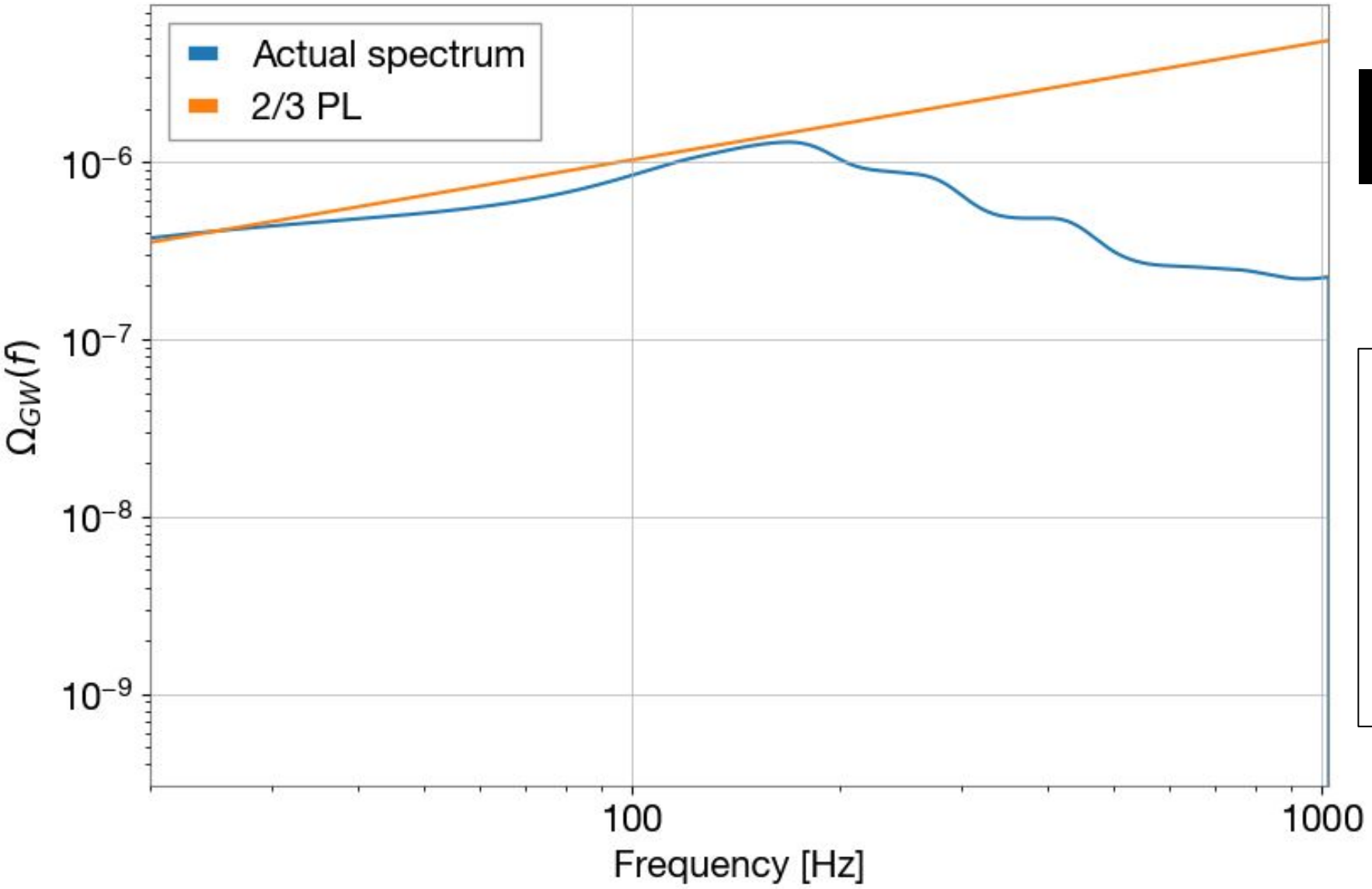

REGIMBAU METHOD

$$\Omega_{GW}(f) \propto \frac{1}{T_{obs}} \sum_{0}^{N} f^3 \frac{dE}{df}$$

$$T_{obs} \propto \sum_{0}^{N} f^3 \frac{dE}{df}$$

Here we have mass distribution that are Log uniform for both mass 1 and mass 2, from 1.5 solar masses to 100 solar masses, 100 injections

INCREASING INJECTIONS

Here we have the following parameters selected:
1. Chirp mass as uniform distribution from 2 to 30 solar masses
2. Luminosity distance from 100 Mpc to 1000 Mpc is used
3. 1000 injections, taken five minutes to run — note the code was streamlined such that 100 injections takes around 1 minute
4. The frequency range is from 20 to 1024 Hz

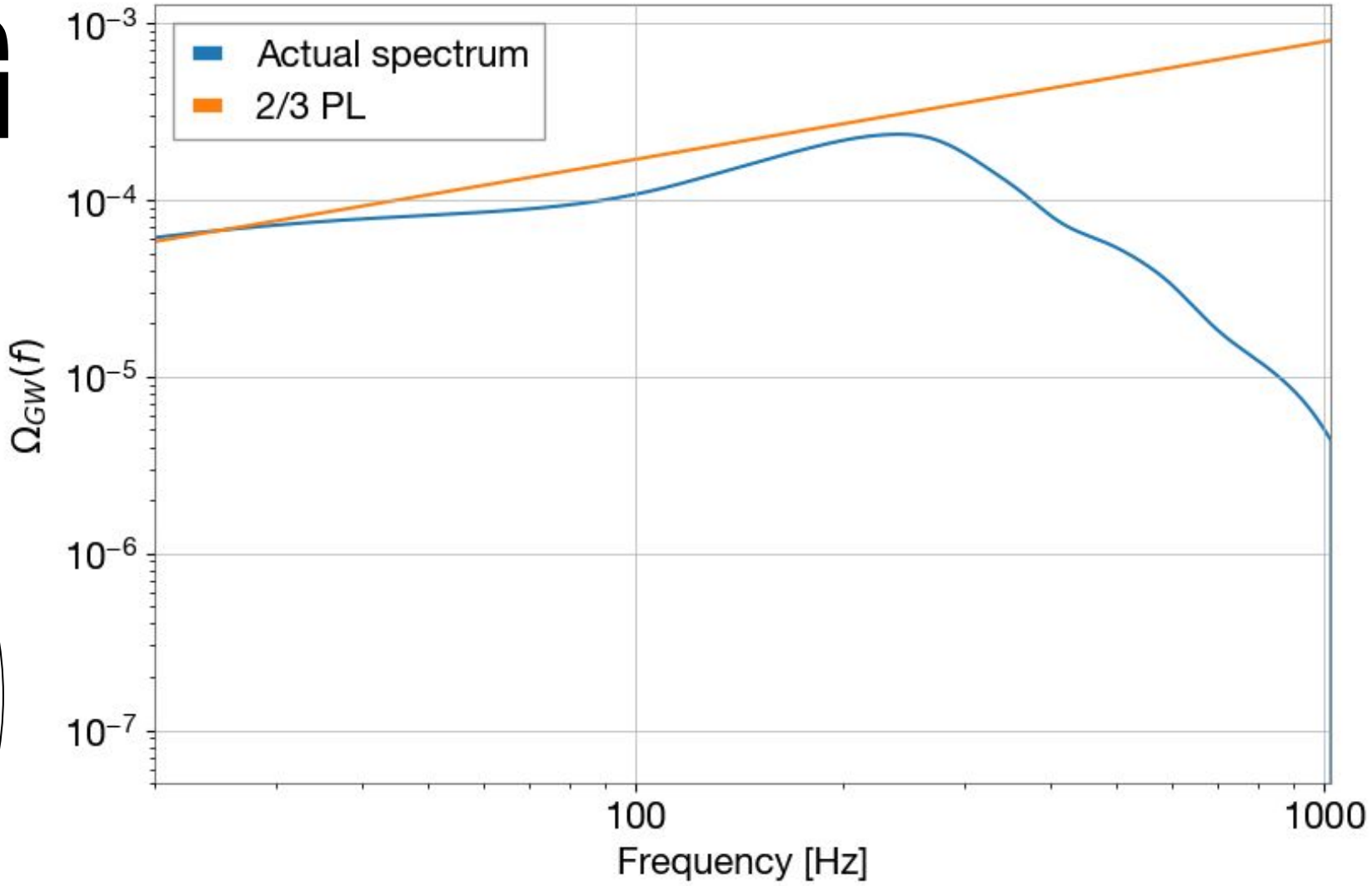

$\frac{1}{N}\sum_{0}^{N} f^3 \frac{dE}{df}$ to normalize, N is number of events

EFFECT OF DIFFERENT REDSHIFT DISTRIBUTIONS

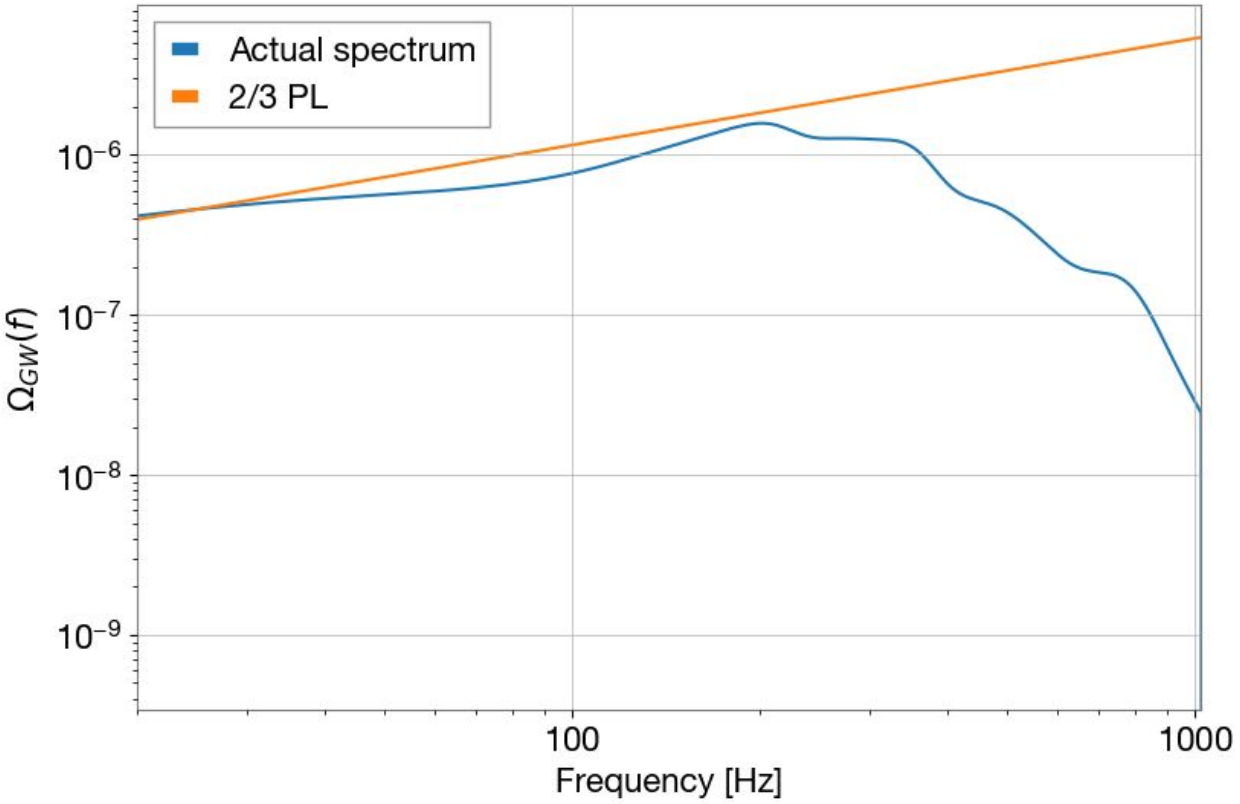

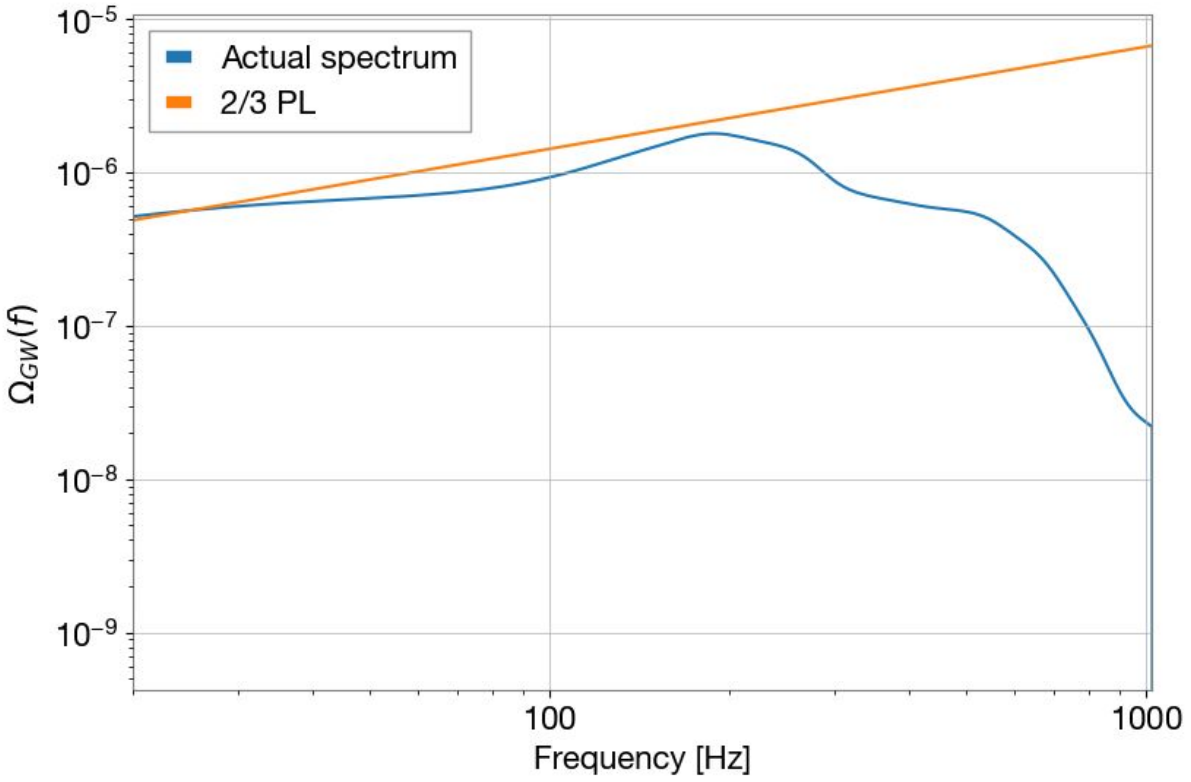

We can make plots for the effect of different redshift limits on Ω(f) against frequency. On the left is a plot generated for redshift of 15 and on the right is a plot generated for a redshift of 10. Both utilize 100 injections.

CALLISTER METHOD

$$\Omega_{GW}(f) = \frac{f}{\rho_c}\frac{d\rho_{GW}}{df} = \frac{f}{\rho_c}\int \frac{R_m(z)}{(1+z)H(z)}\left\langle \frac{dE}{df_s}\right\rangle dz = \frac{f}{\rho_c}\sum_z \left\{\frac{R_m(z)}{(1+z)H(z)}\right\}_z \left\{\left\langle \frac{dE}{df}\right\rangle\right\}_{f,z}$$

$\left\{\left\langle \frac{dE}{df}\right\rangle\right\}_{f,z}$ is the population averaged energy spectrum dependent on frequency and redshift

$$\left\{\left\langle \frac{dE}{df}\right\rangle\right\}_{f,z} = \sum_{m_1, m_2} \{p\}_{m_1, m_2}\left\{\frac{dE}{df}\right\}_{m_1, m_2, f, z}$$

EXAMPLE PLOTS CALLISTER

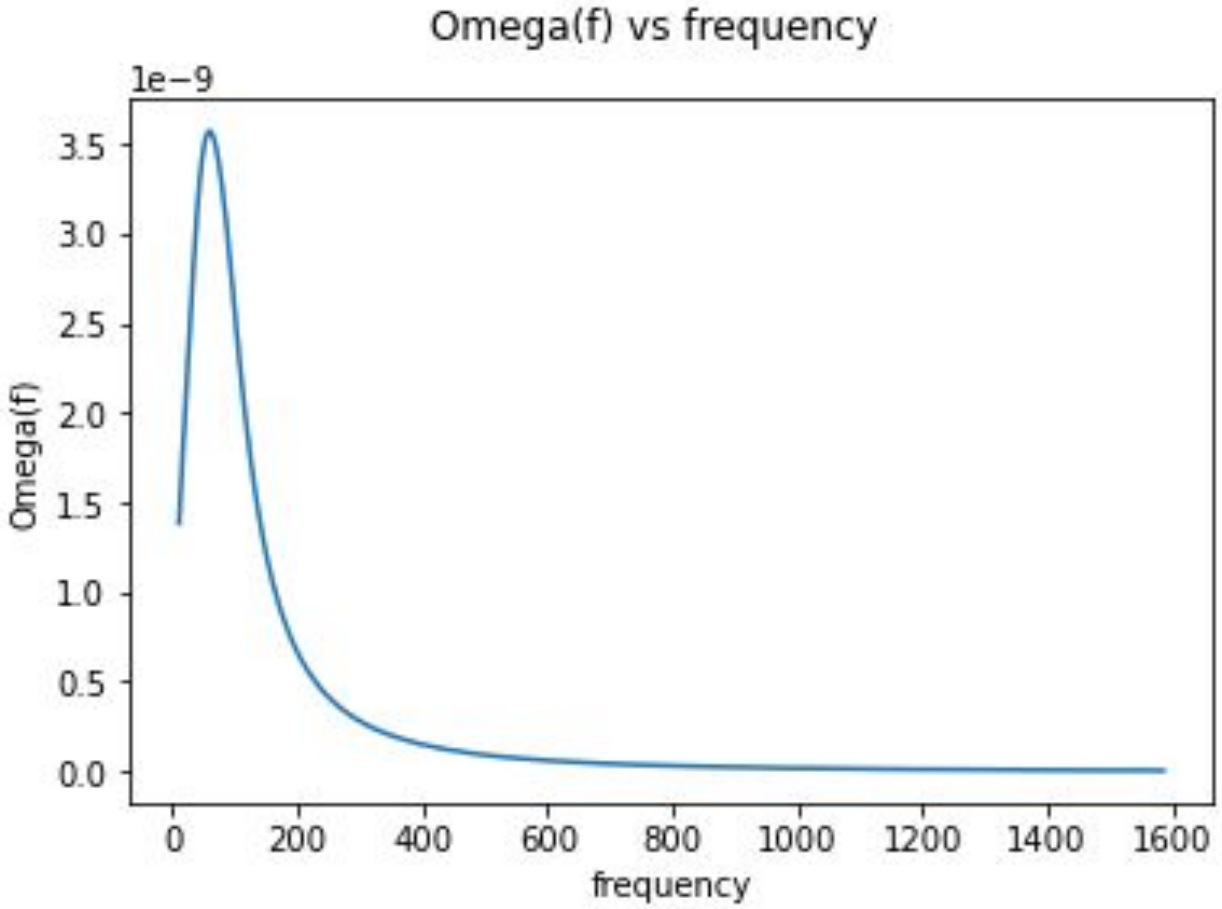

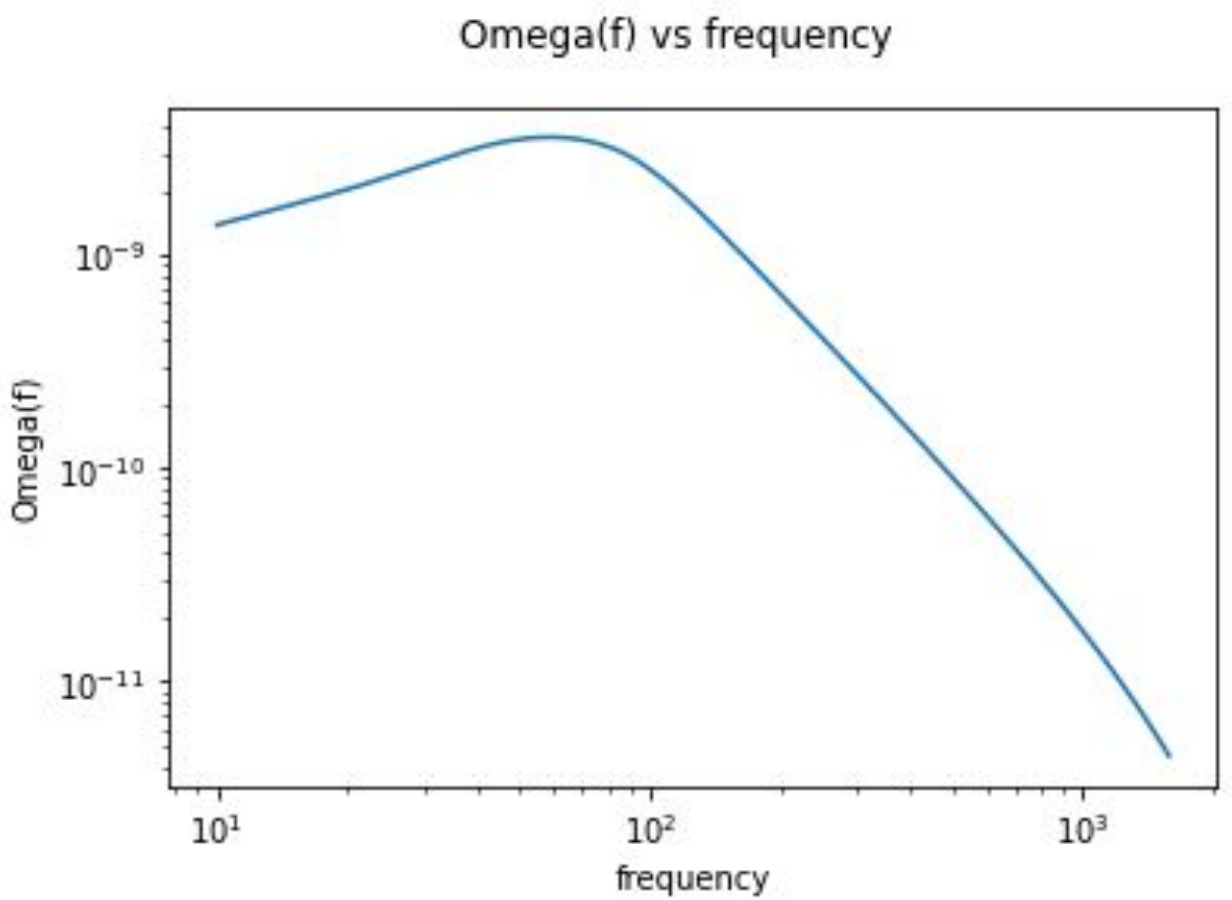

Here, we use the Callister method to create plots for mass distributions. On the left we see linear scale plot for m1_min = 2.5 which corresponds to Minimum BH mass, m1_max = 100 which corresponds to maximum black hole mass. We also utilize m2_min = 1.5, which corresponds to the minimum neutron star mass, and m2_max = 100, which corresponds to the . maximum neutron star mass. We also have the corresponding log scale plot on the right

FREQUENCY VARIATION WITH CHANGES IN MASS DISTRIBUTION

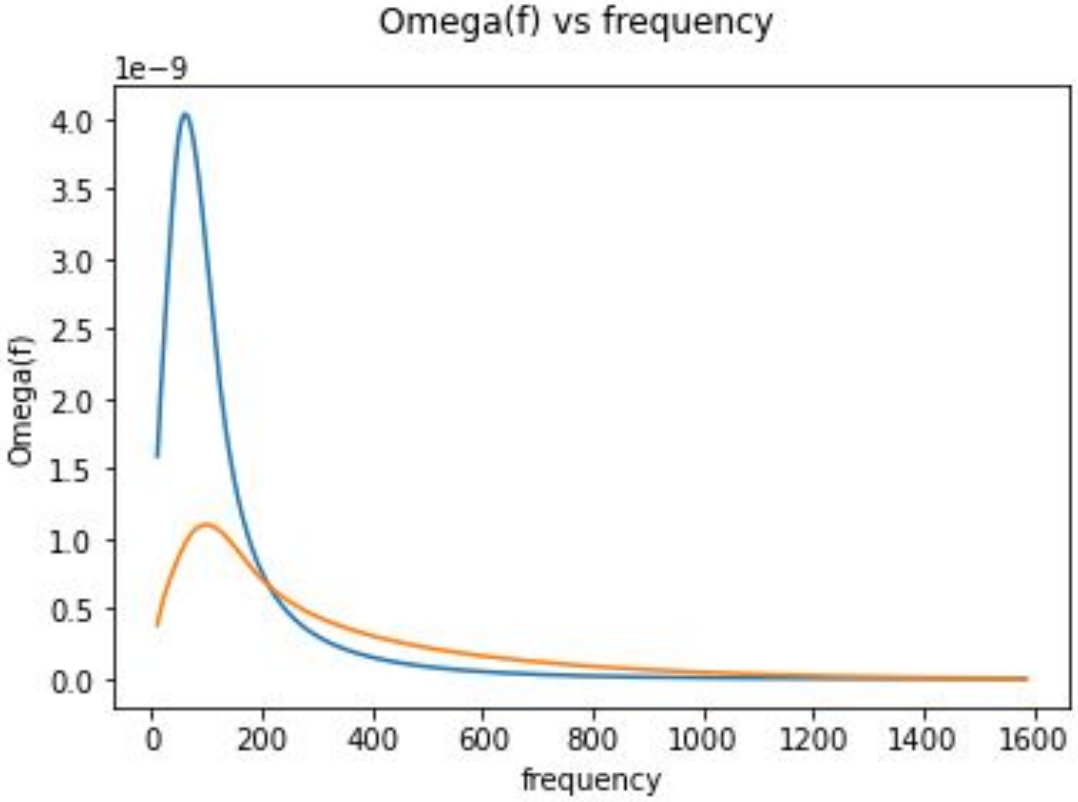

Legend:
O:m1_max = 50
O:m1_max = 100

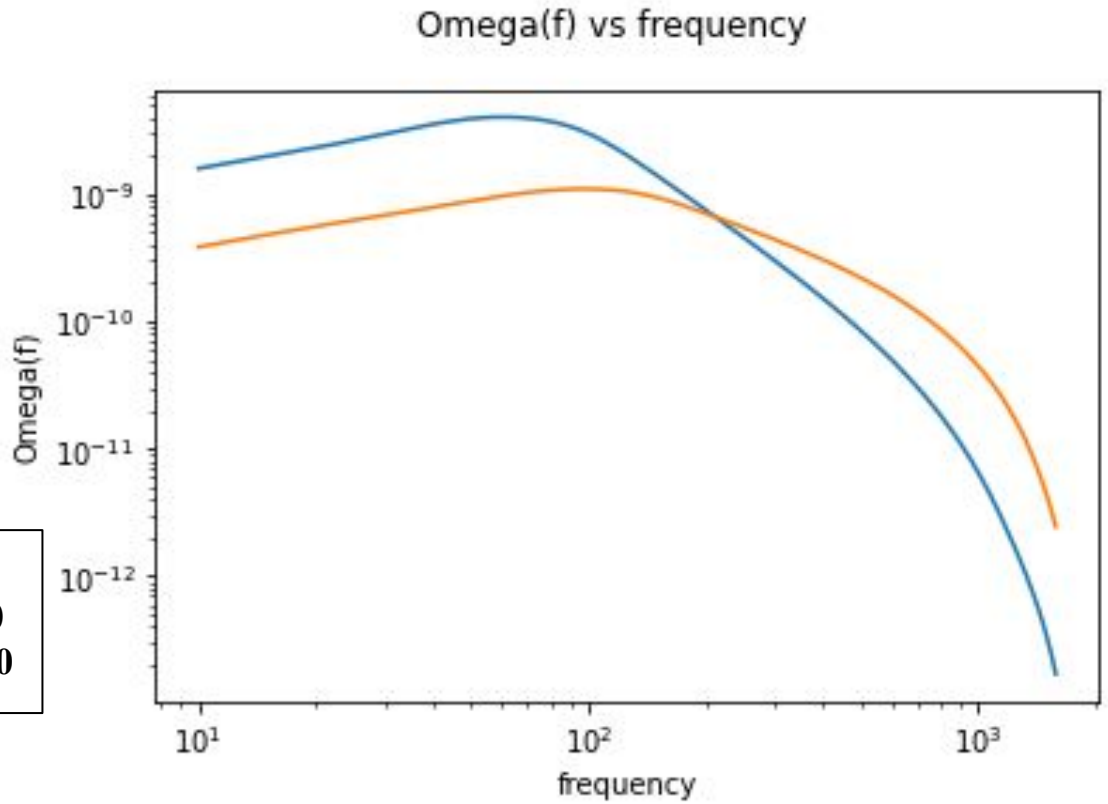

Here, we use the Callister method to create plots for different mass distributions. On the orange plots we see a mass distribution with a minimum of 5 solar masses, maximum of 50 solar masses for the mass of one merging object. On the blue we see plots for a minimum of 5 solar masses, maximum of 100 solar masses for the mass of one merging object. We can see that the peak of the 100-solar-mass maximum plot is shifted to the lower frequencies (clearer on the log scale plot) which is exactly what we expect when we simulate higher mass distributions. In both cases we have a 1:1 mass ratio between merging objects

COMPARISON OF DIFFERENT MASS DISTRIBUTION

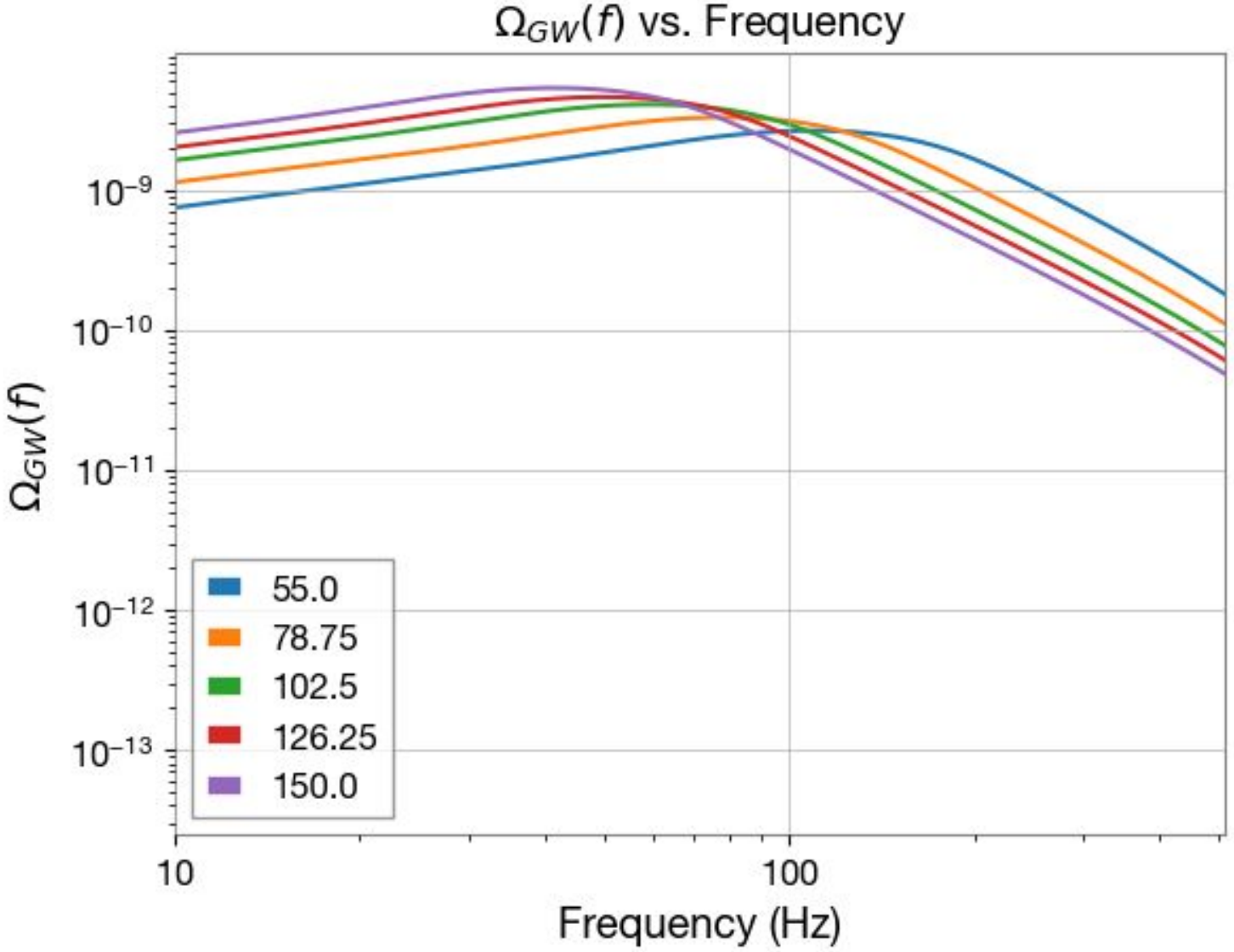

Here we see the application of the callister method for a series of different mass distributions with a 1:1 mass ratio between m1 and m2 but different maximum masses (as shown in the legend), where m1_max = 55, 78.75, etc.

PLOTTING MASS AS X VALUE

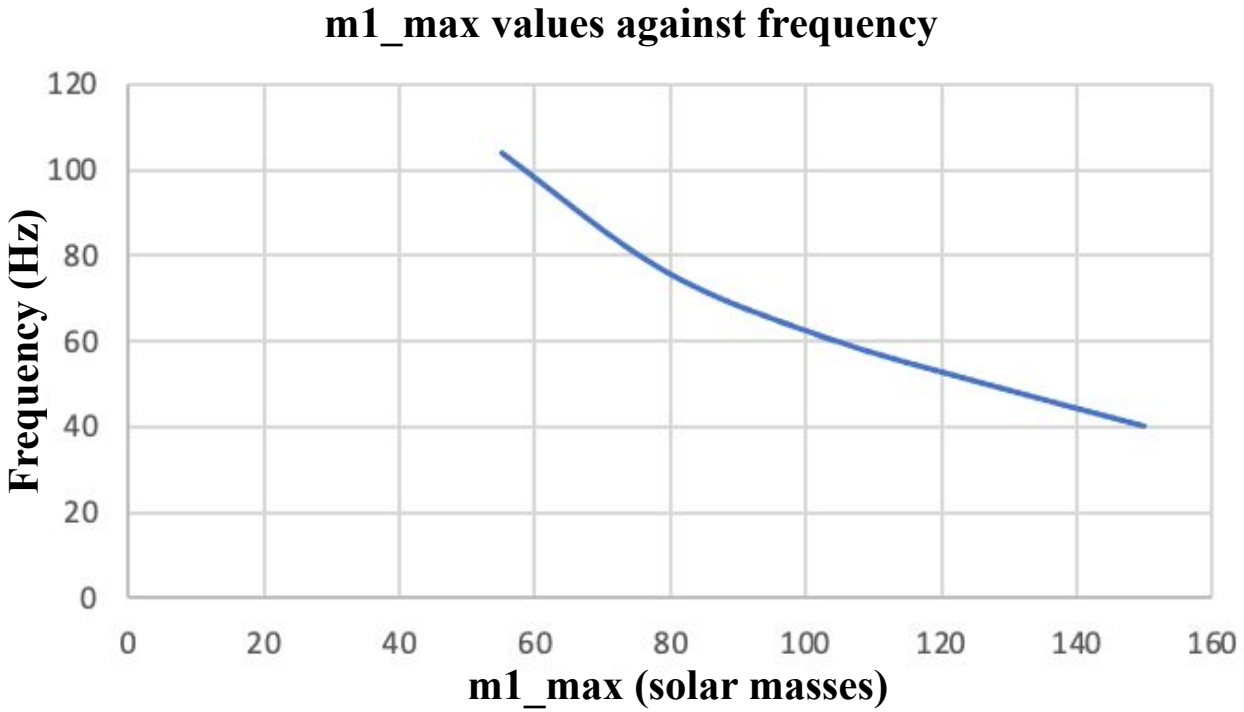

Now, if we take the peak values of the previous graph and for each plot both the frequency at the peak and energy density at peak against maximum mass m1_max on the x axis, we can see the two plots above — one for frequency against mass and the other for energy density against mass.

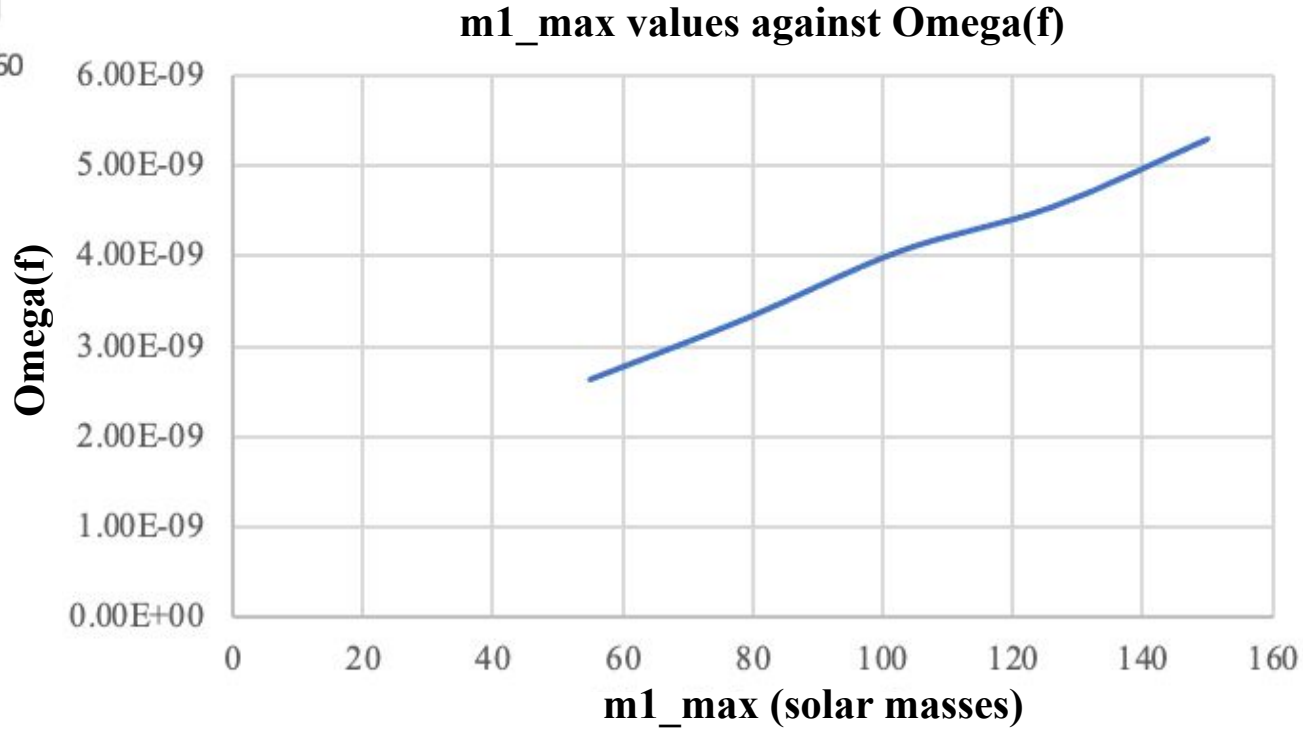

COMPARISON BETWEEN MEAN LOCAL MERGER RATES

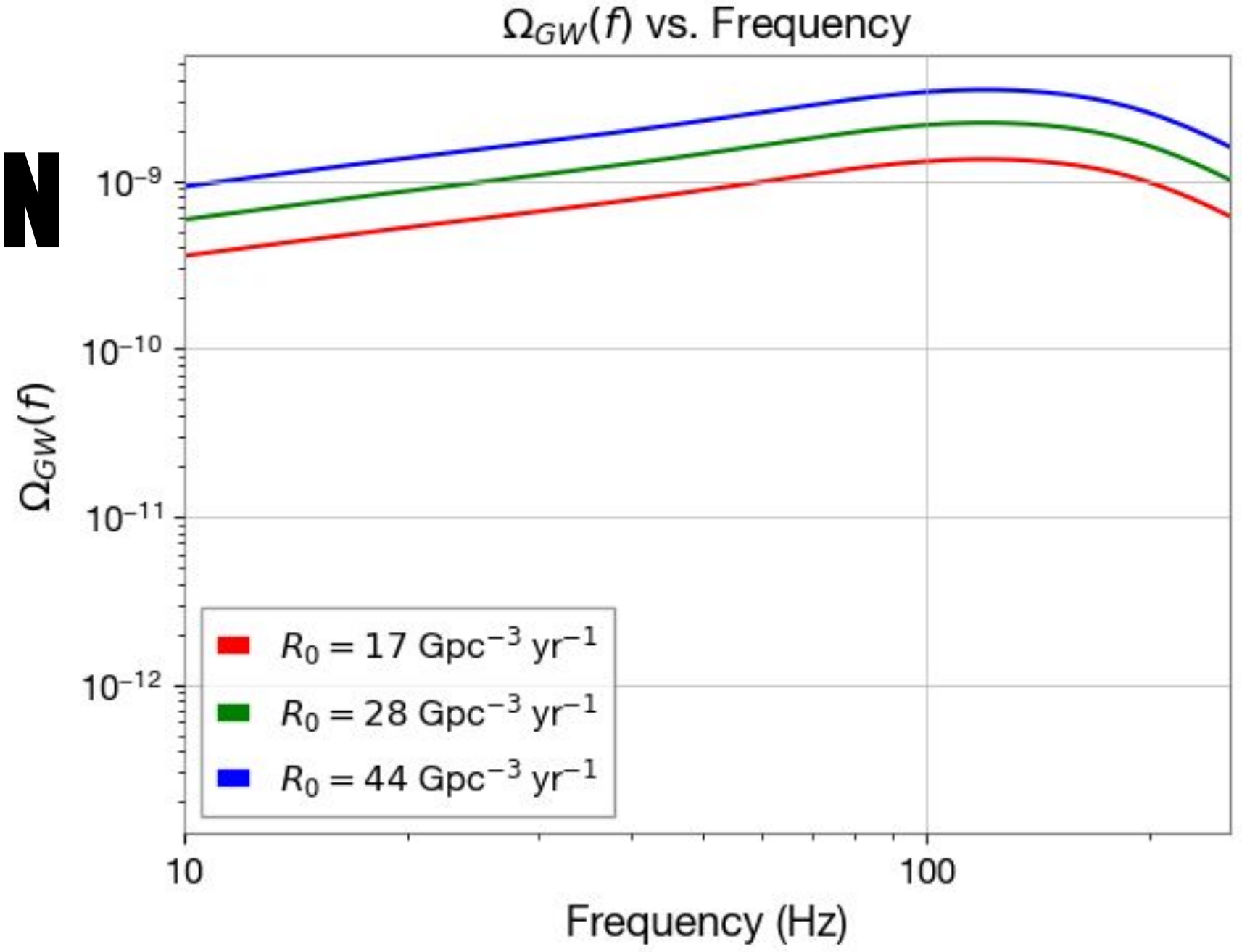

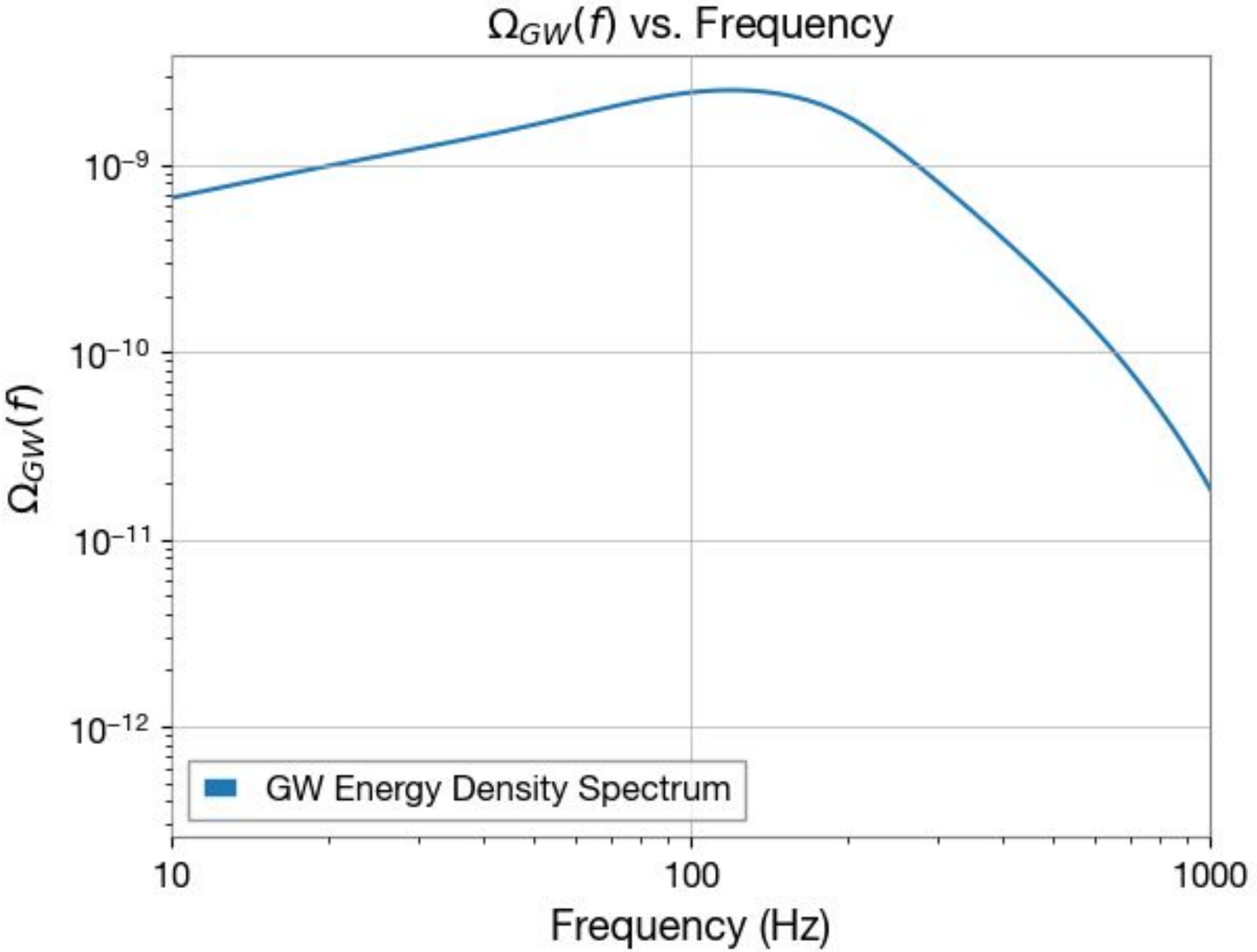

USING REGIMBAU METHOD TO CALCULATE PROBABILITY DISTRIBUTIONS

We can use prior probabilities of both merging masses 1 and 2 and inject these into a probability array to get our probabilities, instead of directly multiplying the change in probability over the mass distribution by a Jacobian.

COMPARISON OF METHODS

We still have the proportionality between observation time and injection number, so we can still try calculating number of injections based on observation time as shown on the right. We can fine tune for certain values of luminosity distance, set a common distribution/observation time of one year, and calculate injections from there. With a common mass distribution of 5 to 50 solar masses, we have the comparison plot.

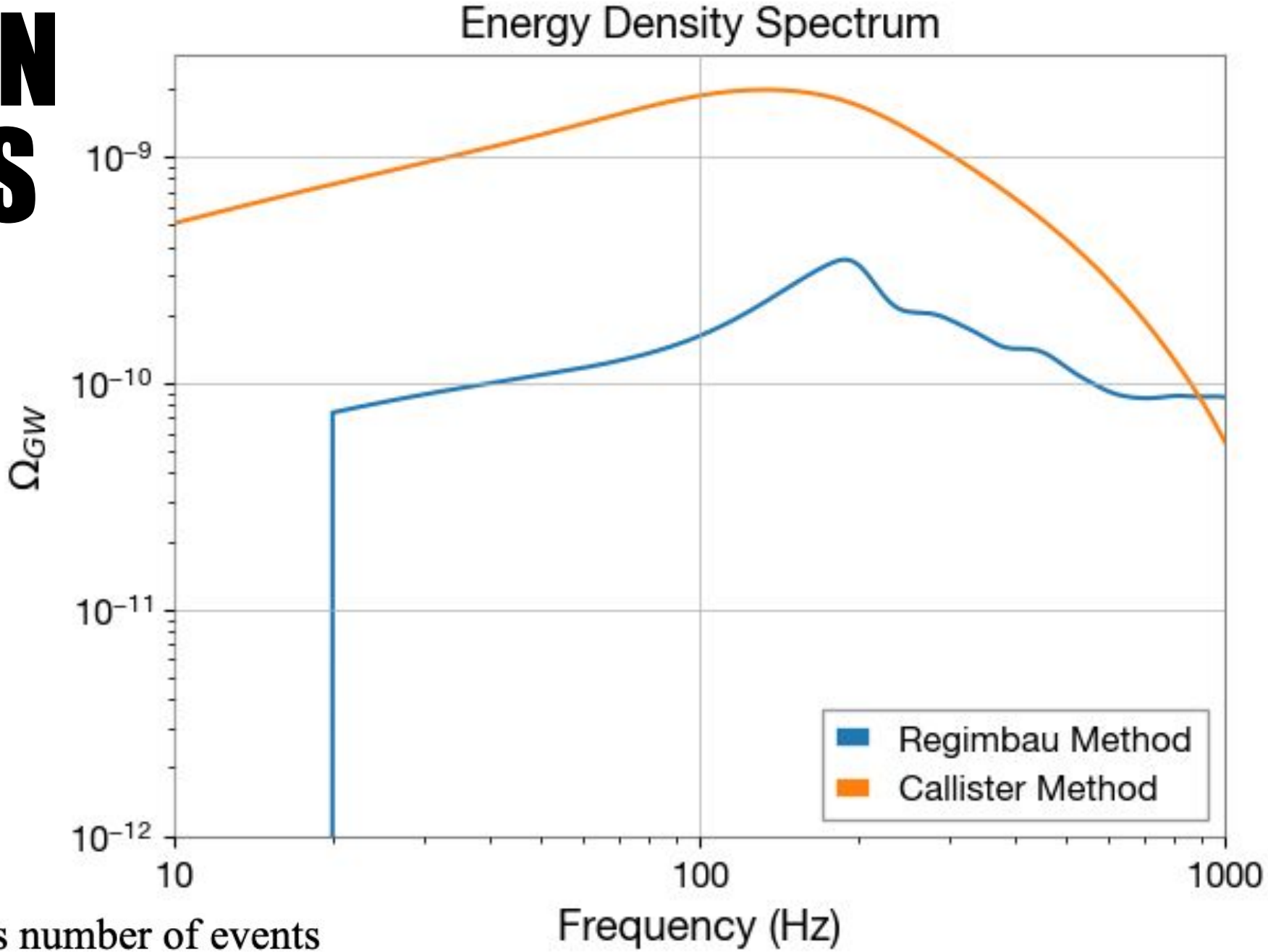

$\frac{1}{N}\sum_{0}^{N} f^3 \frac{dE}{df}$ to normalize, N is number of events

COMPARISON OF METHODS CONTINUED...

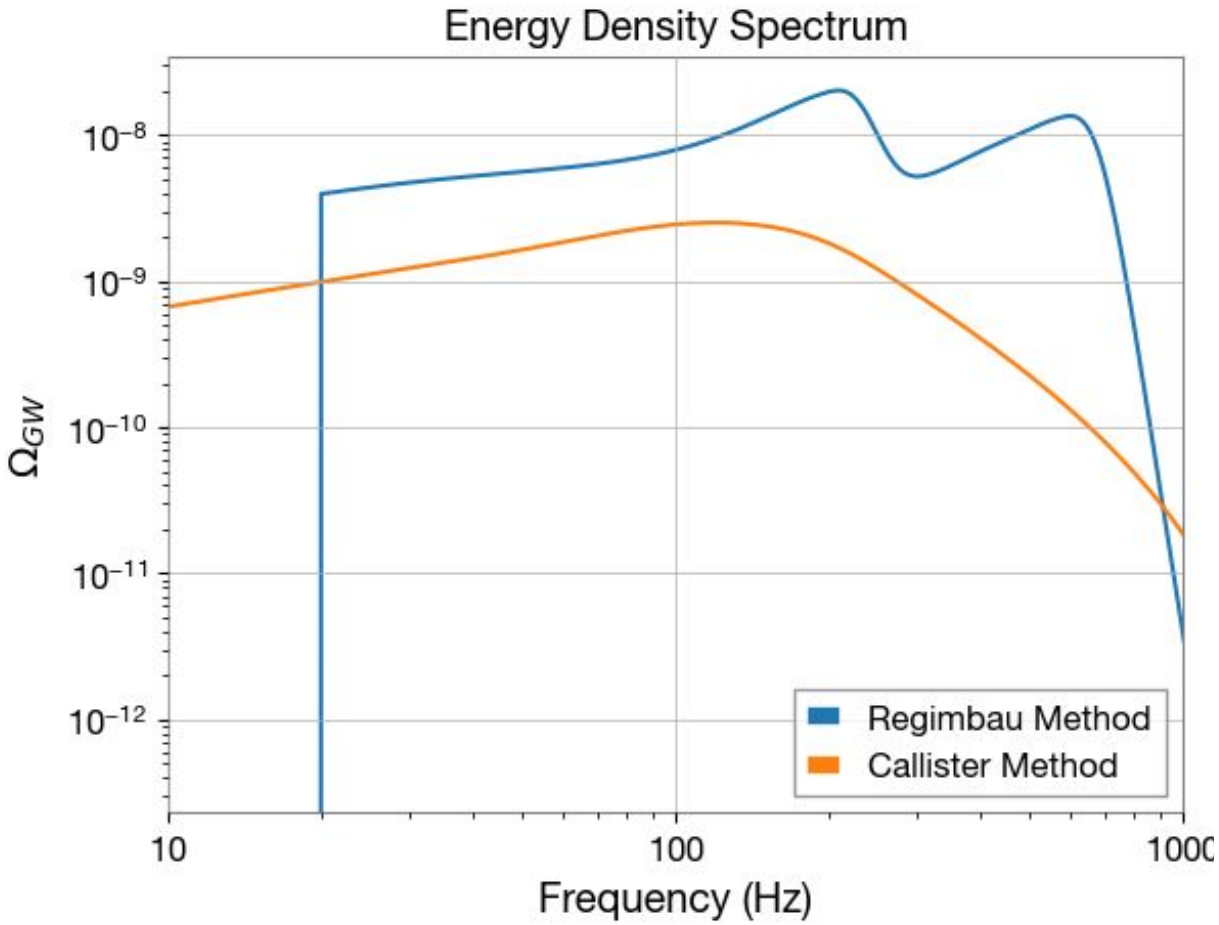

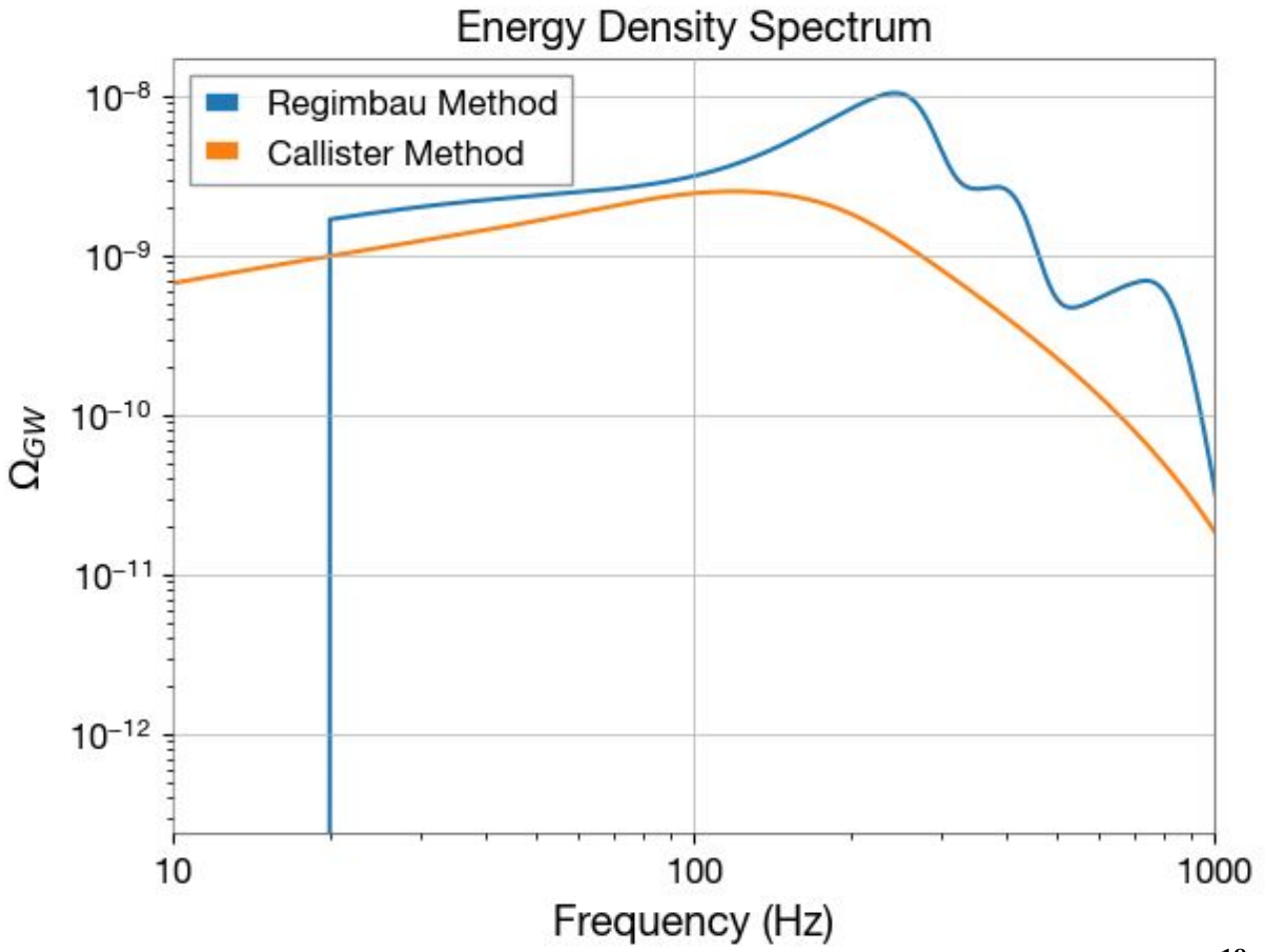

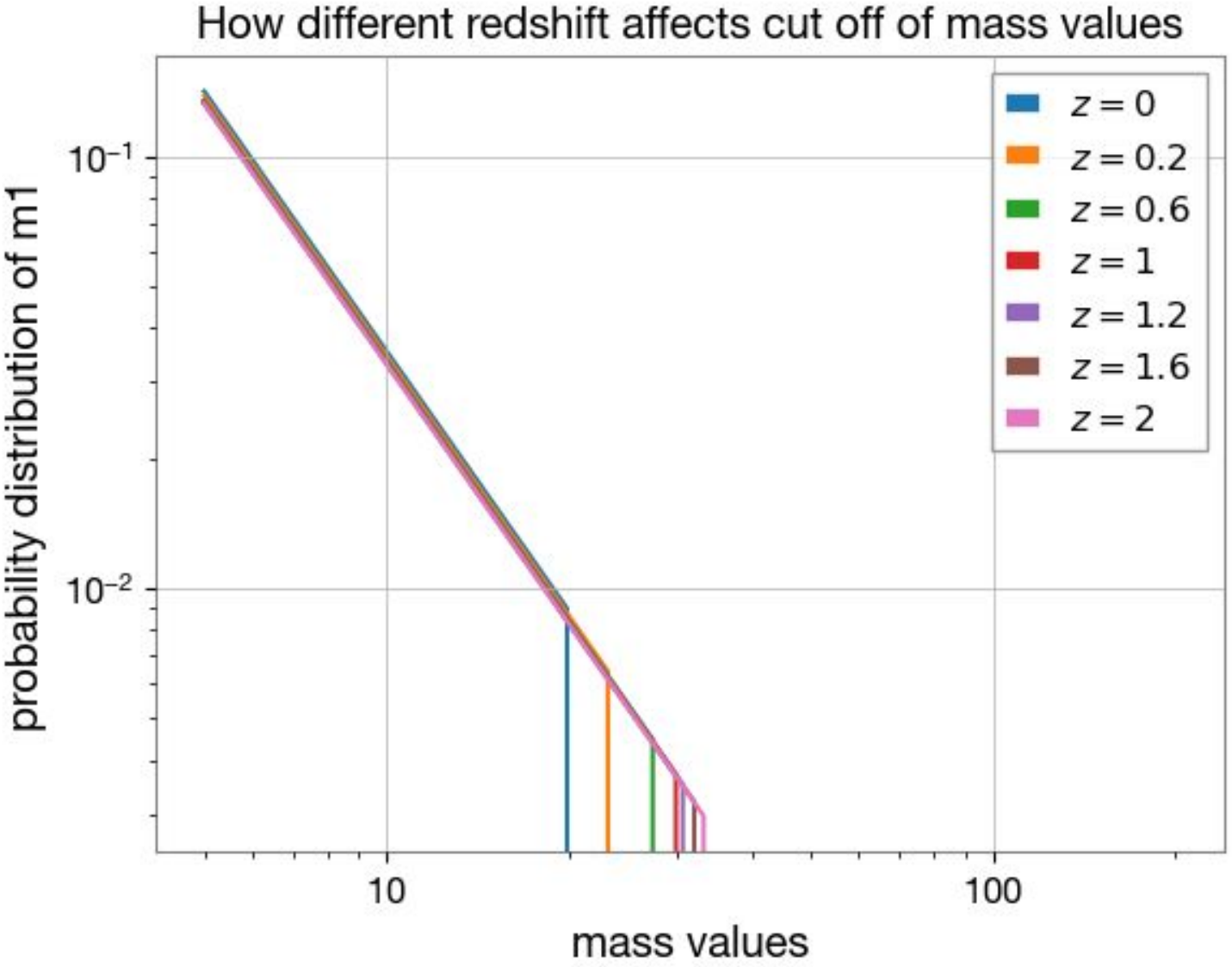

PLOTTING MASS DISTRIBUTIONS AT DIFFERENT REDSHIFTS AGAINST THEIR POWER LAWS

We can plot the mass distribution of mergers — each represented by a single mass of the merging pair — for different redshift values, to see that as we scale mass distribution with redshift, the cut-off value gets larger and larger.

We define the cut off as follows, if we plot the change in mass merger rate with redshift against mass values as a power law, we see there is a point where the change in gradient with change in mass is negligible. The mass value that this occurs at is the cut off of the mass values.

We plot this graph for a red shift of 0 (our reference frame) and a redshift of 2 (corresponding to a knowable change in frequency).

PLOTTING MASS DISTRIBUTIONS AT DIFFERENT REDSHIFTS AGAINST THEIR POWER LAWS

Power law + Peak distribution

$$p(m_1) = m_1^{-\alpha} + ce^{-(m_1 - m_1^*)^2/\delta_{m_1}^2}$$

$$\alpha = \alpha_0 + \alpha^* z$$

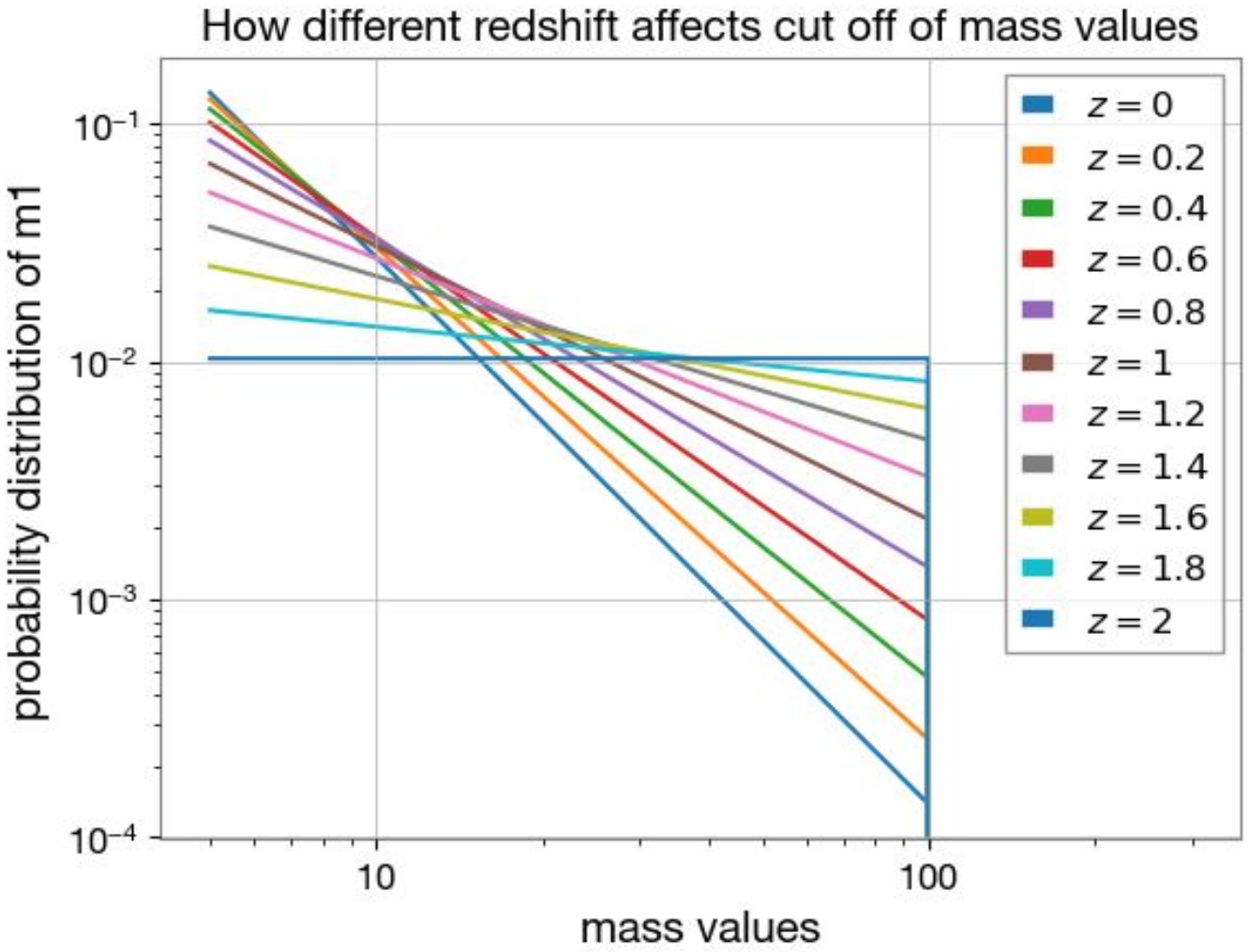

Mass cut off fixed at 100 solar masses

We plot this graph for a red shift of 0 (our reference frame) and a redshift of 2 (corresponding to a knowable change in frequency).

Instead of scaling the cut off for the mass distribution with different red shift values, we can also scale the slope of the mass distribution with different redshift values. This are the alpha values, both the initial alpha_0 and alpha_dot or the change in alpha with change in redshift.

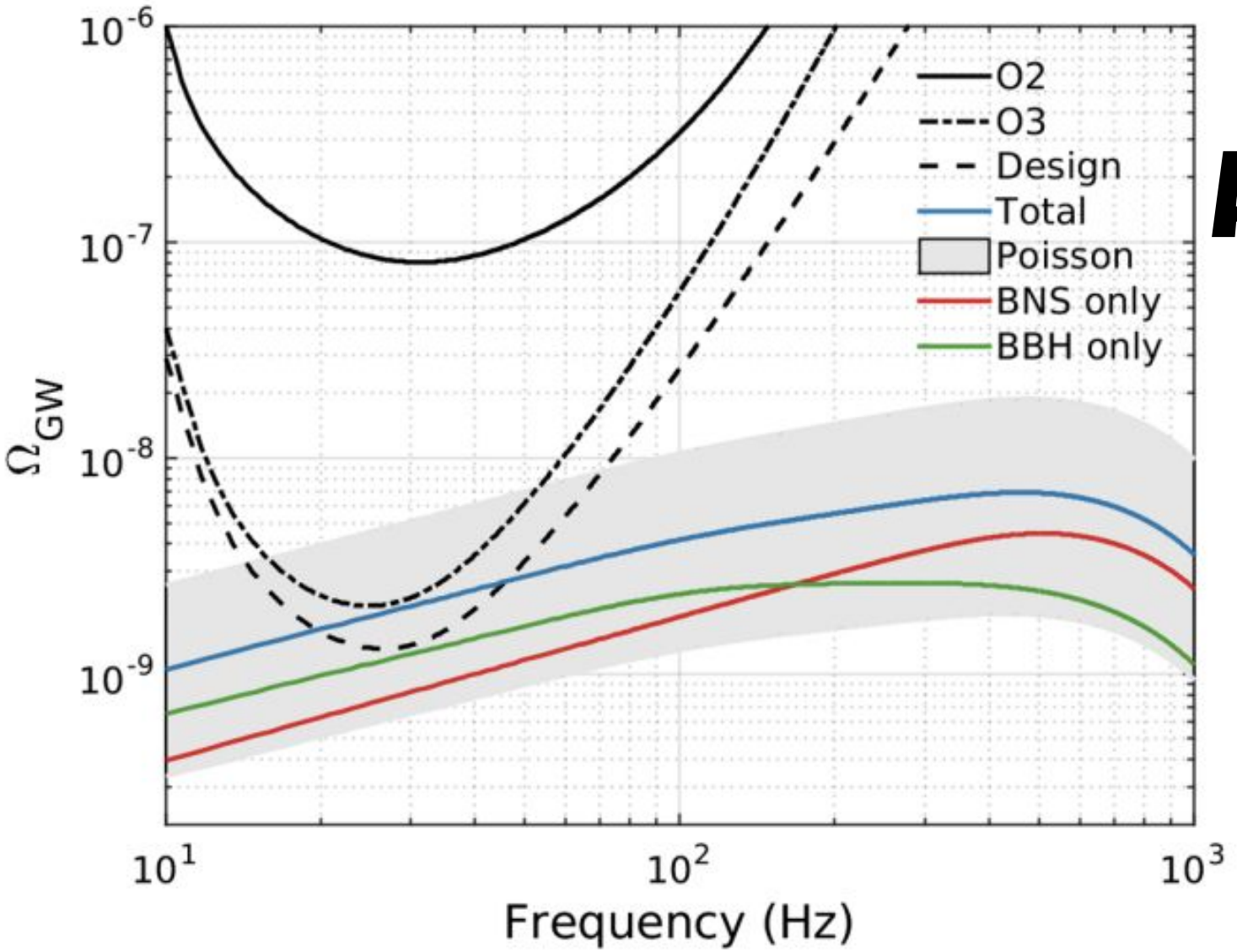

Source: GW170817: *Implications for the Stochastic Gravitational-Wave Background from Compact Binary Coalescences,* B. P. Abbott et al, (LIGO Scientific Collaboration and Virgo Collaboration), *Phys. Rev. Lett,* 120, 091101, Published February 28, 2018, https://journals.aps.org/prl/abstract/10.1103/PhysRevLett.120.091101, Fig 1

CONCLUSION AND THE NEXT STEPS

1. Reproduced and compared the estimates of CBC merger rate and the SGWB using Monte-Carlo sampling and integration (the Regimbau method) and precomputed grids along with probability distributions (the Callister method).

2. Investigated the degree to which these estimates agree with each other and the implications of any discrepancies.

3. Continue to study the dependence of these estimates on uncertainties in the merger rate as a function of mass, redshift distributions of the sources, and potential anisotropies in overall source distribution. Particularly work on new mass distributions on omega.

ACKNOWLEDGEMENTS

- **Mentors:** Alan Weinstein, Patrick Meyers and Arianna Renzini
- Olivia Laske
- LIGO SURF Program, LIGO Lab, and Caltech
- National Science Foundation (NSF)
- Thomas Callister and Arianna Renzini for their code
- Jacob Golomb for his advice

REFERENCES

[1] *LIGO, VIRGO And KAGRA Observing Run Plans*, IGWN, accessed May 2023, https://observing.docs.ligo.org/plan/

[2] *Gravitational Waves from Compact Binary Mergers seen by LIGO and Virgo*, Alan J Weinstein LIGO Laboratory, Caltech for the LIGO and Virgo Collaborations LIGO-Virgo Open Data Workshop, May 27, 2020, https://dcc.ligo.org/public/0168/G2000797/001/Weinstein_CBCs_GWOSC_ODW_20200527.pdf

[3] *Gravitational-wave Transient Catalog (GWTC)*, LVK Collaboration, https://www.gw-openscience.org/eventapi/html/GWTC/

[4] *Stochastic Gravitational-Wave Backgrounds: Current Detection Efforts and Future Prospects,* Renzini, A.I., Goncharov, B., Jenkins, A.C., Meyers, P.M., *Galaxies 2022,* 14 February 2022, https://www.mdpi.com/2075-4434/10/1/34

[5] *Upper limits on the isotropic gravitational-wave background from Advanced LIGO and Advanced Virgo's third observing run*, R. Abbott et al, (LIGO Scientific Collaboration, Virgo Collaboration, and KAGRA Collaboration), *Phys. Rev.* D 104, 022004, Published July 23, 2021, https://journals.aps.org/prd/abstract/10.1103/PhysRevD.104.022004

[6] GW150914: GW150914: *Implications for the Stochastic Gravitational-Wave Background from Binary Black Holes,* B. P. Abbott et al, (LIGO Scientific Collaboration and Virgo Collaboration), *Phys. Rev. Lett.* 116, 131102, Published March 31, 2016, https://journals.aps.org/prl/abstract/10.1103/PhysRevLett.116.131102;

[7]GW170817: *Implications for the Stochastic Gravitational-Wave Background from Compact Binary Coalescences,* B. P. Abbott et al, (LIGO Scientific Collaboration and Virgo Collaboration), *Phys. Rev. Lett,* 120, 091101, Published February 28, 2018, https://journals.aps.org/prl/abstract/10.1103/PhysRevLett.120.091101

[8] *Upper limits on the isotropic gravitational-wave background from Advanced LIGO and Advanced Virgo's third observing run,* R. Abbott et al, (LIGO Scientific Collaboration, Virgo Collaboration, and KAGRA Collaboration), *Phys. Rev. D,* 104, 022004, Published July 23, 2021, https://journals.aps.org/prd/abstract/10.1103/PhysRevD.104.022004, section V.A

[9] *The population of merging compact binaries inferred using gravitational waves through,* GWTC-3, B. P. Abbott et al, (LIGO Scientific Collaboration and Virgo Collaboration), February 23, 2022, https://arxiv.org/abs/2111.03634, section X and Fig 23.

[10] *The stochastic gravitational-wave background from massive black hole binary systems: implications for observations with Pulsar Timing Arrays*, *Monthly Notices of the Royal Astronomical Society*, A. Sesana, A. Vecchio, C. N. Colacino, Volume 390, Issue 1, October 2008, Pages 192-209, https://doi.org/10.1111/j.1365-2966.2008.13682.x

[11] *Introduction To Ligo & Gravitational Waves, Stochastic Gravitational Waves,* LVK Collaboration, https://www.ligo.org/science/GW-Stochastic.php, accessed May 2023

[12] *Impact of a Midband Gravitational Wave Experiment On Detectability of Cosmological Stochastic Gravitational Wave Backgrounds,* Barry C. Barish, Simeon Bird, and Yanou Cui, 16 June 2021, https://arxiv.org/pdf/2012.07874.pdf

[13] *pygwb documentation*, Copyright 2022, Arianna Renzini, Sylvia Biscoveanu, Shivaraj Khandasamy, Kamiel Janssens, Max Lalleman, Katarina Martinovic, Andrew Matas, Patrick Meyers, Alba Romero, Colm Talbot, Leo Tsukada, Kevin Turbang, https://pygwb.docs.ligo.org/pygwb/

THANK YOU